

# Temperature-Dependence of Ultraviolet Absorption Cross-Sections of Alternative Chlorofluoroethanes

DIDIER GILLOTAY<sup>1,2</sup> and PAUL C. SIMON<sup>2</sup>

<sup>1</sup>*Université de Reims-UFRe Sciences, Laboratoire de Spectroscopie atmosphérique et moléculaire, Moulin de la Housse, BP 347, 51062 Reims Cedex, France*

<sup>2</sup>*Institut d'Aéronomie Spatiale de Belgique, Avenue Circulaire 3, B-1180 Bruxelles, Belgium*

(Received: 28 May 1990)

**Abstract.** The absorption cross-sections of HCFC-123 ( $\text{CF}_3\text{—CHCl}_2$ ), HCFC-141b ( $\text{CH}_3\text{—CFCl}_2$ ) and HCFC-142b ( $\text{CH}_3\text{—CF}_2\text{Cl}$ ) are measured between 170 and 250 nm for temperatures ranging from 295 to 210 K with uncertainties between 2 and 4%. They are compared with other available determinations. Temperature effects are discussed and parametrical formulae are proposed to compute the absorption cross-section for wavelengths and temperatures useful in atmospheric modelling calculations. Photodissociation coefficients are presented and their temperature-dependence is discussed.

**Key words:** Alternative hydro-chloro-fluoro-ethanes, UV absorption cross-sections, photodissociation coefficients, temperature-dependence.

## 1. Introduction

It is well known that a key role in the stratospheric ozone budget is played by odd chlorine produced in the stratosphere by photodissociation of halocarbons released in the troposphere. The production of some of these species such as  $\text{CF}_3\text{Cl}$  (CFC-11),  $\text{CF}_2\text{Cl}_2$  (CFC-12),  $\text{C}_2\text{F}_3\text{Cl}_3$  (CFC-113),  $\text{C}_2\text{F}_4\text{Cl}_2$  (CFC-114) and  $\text{C}_2\text{F}_5\text{Cl}$  (CFC-115) has been recently limited by the 'Montreal Protocol on substances that deplete the ozone layer' because of their high ozone depletion potential.

New products are currently under study to replace the most commonly used chlorofluorocarbons in many applications. Among them, partially hydrogenated halocarbons are relatively easily destroyed by OH radicals in the troposphere and their lifetime is consequently much shorter than those that are fully halogenated (Gillotay *et al.*, 1989a) which are mainly dissociated by the solar radiation in the stratosphere and, to a very low extent, by reaction with O<sup>1</sup>D.

The purpose of this paper is to report measurements of the temperature-dependence of the ultraviolet absorption cross-sections of three hydrogen-containing chlorofluoroethanes ( $\text{CH}_3\text{—CF}_2\text{Cl}$  (HCFC-142b),  $\text{CH}_3\text{—CFCl}_2$  (HCFC-141b), and  $\text{CF}_3\text{—CHCl}_2$  (HCFC-123)) performed between 170 and 250 nm, for tem-

peratures ranging from 295 to 210 K. These data are used to estimate the temperature-dependence of their photodissociation coefficients relative to those calculated at room temperature.

## 2. Experimental

Ultraviolet absorption cross-sections and their temperature-dependence were determined by means of the experimental device previously described by Gillotay *et al.* (1989b) which includes a deuterium lamp, a 1 m McPherson 225 monochromator, a beam splitter, 200 cm and 20 cm thermostated absorption cells (one of the cells being the reference channel), EMR type 542 P-09-18 solar blind photomultipliers, and a data acquisition system.

The wavelength scanning is performed by means of a stepping motor. An increment of 1 nm is usually used for a continuum spectrum. The band width is 0.1 nm and the wavelength repeatability  $\pm 0.01$  nm. The pressure inside the cell, ranging from  $2 \times 10^{-3}$  to  $1 \times 10^3$  Torr, is measured by means of three capacitance MKS-Baratron manometers 170–315 with a 1, 10, and 1000 Torr full-scale range. The calibration of these manometers takes into account local pressure measurements at regular intervals and allows a precision better than 0.1%.

Low temperatures are measured with absolute uncertainties of around  $\pm 1$  K by means of five Pt100 temperature sensors (a low temperature stability of  $\pm 0.3$  K is usually observed). The mean of the five temperatures measured by the sensors is representative, within  $\pm 1$  K, of the temperature determined from the perfect gas law.

The three compounds have, respectively, purities of 99.99% for HCHC-142b, 99.72% for HCFC-141b, and 98.4% for HCFC-123, as determined by gas-phase chromatography before and after the sampling procedure. Adequate corrections are made in the determination of the absorption cross-sections of HCFC-123, taking into account the mixing ratio and the published cross-sections of the impurities, namely  $\text{CFCl}_3$  (0.77%) and  $\text{C}_2\text{F}_4\text{Cl}_2$  (0.48%).

Table I. Experimental conditions

Compound	$T$ (K)	Pressure range (Torr)	No. of rec.
HCFC-123	295	239.5–0.0625	118
	248	13.55–0.0425	62
	210	3.25–0.0320	38
HCFC-141b	295	204.0–0.117	99
	245	6.00–0.0286	66
	215	3.63–0.0250	42
HCFC-142b	295	759.2–0.241	58
	245	317.2–0.184	54
	215	34.73–0.151	70

The determination of the absorption cross-sections is made after sequential recordings of incident and transmitted radiation fluxes, measured under the same temperature conditions, using the Beer—Lambert law. The experimental conditions are summarised in Table I.

In order to obtain data only in the range where the Beer—Lambert law is still applicable, only that having transmission values of between 10 and 85% are considered for the determination of the absorption cross-section, for a given pressure in the cell.

Figure 1 illustrates the absorption cross-section values obtained at one pressure from the full range of transmission. These values are compared with those obtained using the limited range of transmission, described above, at different pressures. The departure from the Beer—Lambert law is well illustrated when transmission is above 90%.

### 3. Results

Numerical values of absorption cross-sections, interpolated from the experimental determinations are given for selected wavelengths (2 nm intervals and  $500\text{ cm}^{-1}$  wavenumber intervals) in Tables IIa—IVa and IIb—IVb within the experimental accuracy defined below. Wavelengths are defined in vacuum.

According to the experimental conditions and the previously published error

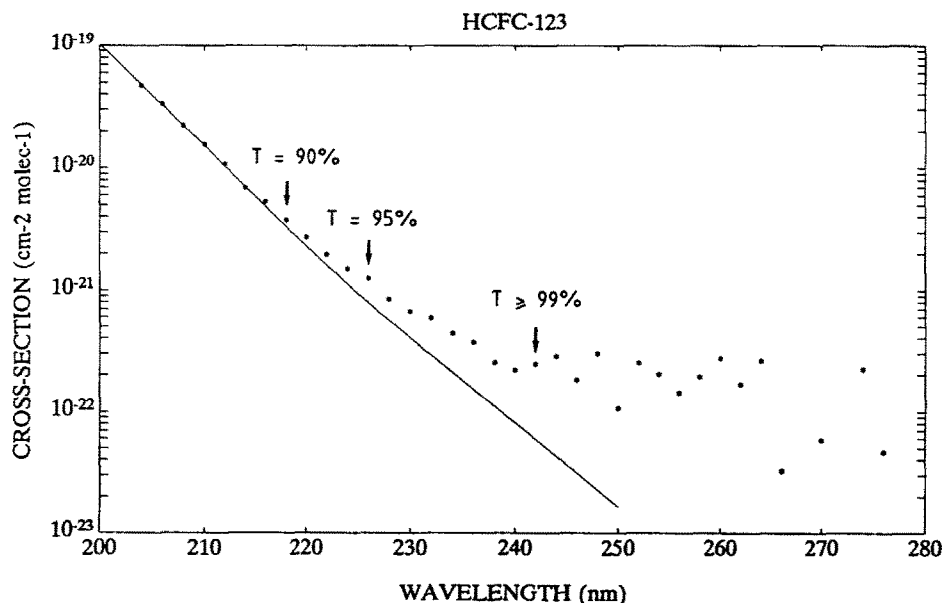


Fig. 1. Comparison between absorption cross-section values obtained for one pressure condition with an unlimited range of transmitted fluxes ( $\bullet$ ), and for various pressure conditions considering the limited range of transmitted fluxes (—).

budget (Simon *et al.*, 1988a), the values given in Tables IIa–IVa and IIb–IVb are determined to within an accuracy of  $\pm 2\%$  at room temperature and around  $\pm 3\%$  at low temperatures.

Table IIa. Absorption cross-sections of HCFC-123 ( $\text{CF}_3\text{—CHCl}_2$ ) at 2 nm intervals for five selected temperatures (295, 270, 250, 230, 210 K)

Wavelength $\lambda(\text{nm})$	$\sigma(\lambda) \times 10^{21} (\text{cm}^2 \text{ molec.}^{-1})$				
	295 K	270 K	250 K	230 K	210 K
170	1747	1767	1783	1799	1815
172	1935	1959	1978	1997	2017
174	2024	2046	2063	2080	2098
176	2010	2023	2034	2044	2055
178	1901	1903	1904	1905	1907
180	1720	1709	1701	1692	1684
182	1496	1474	1456	1439	1422
184	1254	1224	1201	1178	1155
186	1017	983	957	931	905
188	802	767	740	713	688
190	616	582	557	533	509
192	462	433	410	389	368
194	341	315	296	278	261
196	247	226	210	196	182
198	176	159	147	136	126
200	124	111	102	93.5	85.7
202	86.9	77.2	70.2	63.8	58.0
204	60.4	53.2	48.0	43.3	39.0
206	41.8	36.4	32.7	29.3	26.2
208	28.8	24.9	22.2	19.8	17.6
210	19.9	17.1	15.1	13.3	11.8
212	13.7	11.7	10.3	9.03	7.94
214	9.47	8.01	7.01	6.13	5.36
216	6.57	5.52	4.80	4.18	3.63
218	4.58	3.82	3.31	2.86	2.47
220	3.21	2.66	2.29	1.97	1.69
222	2.26	1.86	1.59	1.36	1.17
224	1.61	1.31	1.12	0.951	0.809
226	1.15	0.934	0.789	0.667	0.564
228	0.832	0.668	0.561	0.471	0.395
230	0.605	0.482	0.401	0.334	0.278
232	0.444	0.350	0.288	0.238	0.196
234	0.329	0.255	0.209	0.170	0.139
236	0.245	0.188	0.152	0.122	0.0987
238	0.184	0.139	0.110	0.0879	0.0700
240	0.140	0.103	0.0806	0.0632	0.0495
242	0.106	0.0766	0.0589	0.0453	0.0349
244	0.0815	0.0572	0.0430	0.0324	0.0244
246	0.0628	0.0427	0.0314	0.0230	0.0169
248	0.0484	0.0318	0.0227	0.0162	0.0116
250	0.0375	0.0236	0.0164	0.0113	0.00783

Table IIb. Absorption cross-sections of HCFC-123 ( $\text{CF}_3\text{—CHCl}_2$ ) averaged over the spectral intervals of  $500\text{ cm}^{-1}$  used in atmospheric modelling calculations for five selected temperatures (295, 270, 250, 230, 210 K)

No.	Wavelength (nm)	$\sigma(\lambda) \times 10^{21}$ ( $\text{cm}^2\text{ molec.}^{-1}$ )				
		295 K	270 K	250 K	230 K	210 K
43	169.5–172.4	1848	1870	1888	1906	1925
44	172.4–173.9	1999	2022	2041	2060	2079
45	173.9–175.4	2031	2050	2066	2081	2097
46	175.4–177.0	2003	2015	2025	2035	2045
47	177.0–178.6	1915	1918	1921	1923	1926
48	178.6–180.2	1780	1773	1768	1762	1756
49	180.2–181.8	1612	1595	1582	1569	1556
50	181.8–183.5	1418	1393	1373	1354	1339
51	183.5–185.2	1212	1181	1156	1133	1110
52	185.2–186.9	1012	977	951	925	900
53	186.9–188.7	822	787	760	734	708
54	188.7–190.5	659	625	599	574	550
55	190.5–192.3	505	474	450	428	407
56	192.3–194.2	383	355	335	316	298
57	194.2–196.1	283	260	244	228	213
58	196.1–198.0	207	188	175	162	150
59	198.0–200.0	148	133	123	113	104
60	200.0–202.0	104	92.8	84.7	77.3	70.6
61	202.0–204.1	71.9	63.5	57.5	52.1	47.2
62	204.1–206.2	48.9	42.8	38.5	34.6	31.1
63	206.2–208.3	33.1	28.8	25.7	22.9	20.4
64	208.3–210.5	22.2	19.1	16.9	15.0	13.3
65	210.5–212.8	14.6	12.5	11.0	9.67	8.51
66	212.8–215.0	9.65	8.16	7.14	6.25	5.47
67	215.0–217.4	6.34	5.32	4.62	4.02	3.49
68	217.4–219.8	4.11	3.43	2.96	2.56	2.21
69	219.8–222.2	2.69	2.22	1.91	1.64	1.41
70	222.2–224.7	1.77	1.45	1.23	1.05	0.894
71	224.7–227.3	1.15	0.934	0.789	0.667	0.564
72	227.3–229.9	0.755	0.605	0.507	0.424	0.355
73	229.9–232.6	0.498	0.394	0.326	0.270	0.224
74	232.6–235.3	0.331	0.257	0.210	0.172	0.140
75	235.3–238.1	0.222	0.169	0.136	0.109	0.0875
76	238.1–241.0	0.150	0.111	0.0872	0.0686	0.0540
77	241.0–243.9	0.100	0.0718	0.0549	0.0421	0.0322
78	243.9–246.9	0.0679	0.0466	0.0345	0.0255	0.0189
79	246.9–250.0	0.0454	0.0295	0.0209	0.0148	0.0105
80	250.0–253.2	0.0309	0.0189	0.0127	0.00856	0.00576

Table IIIa. Absorption cross-sections of HCFC-141b ( $\text{CF}_3\text{—CFCl}_2$ ) at 2 nm intervals for five selected temperatures (295, 270, 250, 230, 210 K)

Wavelength $\lambda$ (nm)	$\sigma(\lambda) \times 10^{21}$ (cm <sup>2</sup> molec. <sup>-1</sup> )				
	295 K	270 K	250 K	230 K	210 K
170	1431	1428	1418	1409	1399
172	1451	1451	1452	1452	1452
174	1542	1549	1556	1562	1568
176	1629	1655	1675	1696	1717
178	1726	1763	1792	1822	1852
180	1723	1762	1794	1826	1858
182	1629	1662	1690	1718	1746
184	1464	1488	1507	1526	1546
186	1257	1270	1279	1289	1299
188	1036	1038	1039	1040	1042
190	822	816	811	806	801
192	631	620	612	603	595
194	470	458	448	438	428
196	341	329	319	309	300
198	242	231	222	214	206
200	168	159	152	145	138
202	115	108	102	96.7	91.7
204	77.5	71.9	67.7	63.7	60.0
206	51.6	47.5	44.4	41.6	38.9
208	34.0	31.1	28.9	26.9	25.0
210	22.3	20.2	18.7	17.3	16.0
212	14.5	13.1	12.0	11.1	10.2
214	9.40	8.42	7.72	7.07	6.48
216	6.08	5.42	4.94	4.50	4.10
218	3.93	3.48	3.16	2.86	2.60
220	2.54	2.23	2.02	1.82	1.64
222	1.64	1.43	1.29	1.15	1.03
224	1.07	0.922	0.820	0.730	0.650
226	0.693	0.593	0.523	0.461	0.407
228	0.452	0.381	0.333	0.290	0.253
230	0.296	0.245	0.211	0.182	0.156
232	0.194	0.158	0.133	0.113	0.0957
234	0.128	0.101	0.0840	0.0697	0.0579
236	0.0841	0.0647	0.0525	0.0425	0.0345
238	0.0556	0.0412	0.0325	0.0256	0.0202
240	0.0368	0.0261	0.0199	0.0151	0.0115

Table IIIb. Absorption cross-sections of HCFC-141b ( $\text{CH}_3\text{—CFCl}_2$ ) averaged over the spectral intervals of  $500\text{ cm}^{-1}$  used in atmospheric modelling calculations for five selected temperatures (295, 270, 250, 230, 210 K)

No.	Wavelength (nm)	$\sigma(\lambda) \times 10^{21}$ ( $\text{cm}^2\text{ molec.}^{-1}$ )				
		295 K	270 K	250 K	230 K	210 K
43	169.5–172.4	1426	1424	1421	1417	1414
44	172.4–173.9	1501	1504	1507	1510	1513
45	173.9–175.4	1570	1583	1593	1603	1614
46	175.4–177.0	1640	1666	1688	1710	1732
47	177.0–178.6	1720	1755	1784	1813	1843
48	178.6–180.2	1736	1775	1806	1838	1871
49	180.2–181.8	1686	1723	1753	1784	1815
50	181.8–183.5	1582	1612	1637	1663	1689
51	183.5–185.2	1430	1452	1469	1487	1505
52	185.2–186.9	1252	1264	1273	1283	1293
53	186.9–188.7	1058	1061	1063	1065	1067
54	188.7–190.5	874	870	866	862	859
55	190.5–192.3	686	676	668	660	653
56	192.3–194.2	527	515	505	495	486
57	194.2–196.1	392	379	369	360	350
58	196.1–198.0	286	274	264	255	247
59	198.0–200.0	202	192	184	176	169
60	200.0–202.0	139	131	125	119	113
61	202.0–204.1	93.6	87.2	82.4	77.8	73.5
62	204.1–206.2	61.4	56.7	53.2	49.9	46.8
63	206.2–208.3	39.8	36.5	34.0	31.7	29.5
64	208.3–210.5	25.3	23.0	21.3	19.8	18.3
65	210.5–212.8	15.6	14.1	13.0	12.0	11.0
66	212.8–215.0	9.60	8.61	7.89	7.23	6.62
67	215.0–217.4	5.82	5.18	4.72	4.30	3.92
68	217.4–219.8	3.44	3.05	2.76	2.50	2.26
69	219.8–222.2	2.04	1.79	1.61	1.45	1.30
70	222.2–224.7	1.20	1.04	0.928	0.828	0.738
71	224.7–227.3	0.693	0.593	0.523	0.461	0.407
72	227.3–229.9	0.398	0.334	0.290	0.252	0.219
73	229.9–232.6	0.227	0.186	0.159	0.135	0.115
74	232.6–235.3	0.129	0.102	0.0849	0.0706	0.0586
75	235.3–238.1	0.0728	0.0553	0.0444	0.0357	0.0286
76	238.1–241.0	0.0408	0.0293	0.0225	0.0173	0.0133

Table IVa. Absorption cross-sections of HCFC-142b ( $\text{CH}_3\text{—CF}_2\text{Cl}$ ) at 2 nm intervals for five selected temperatures (295, 270, 250, 230, 210 K)

Wavelength $\lambda$ (nm)	$\sigma(\lambda) \times 10^{21}$ ( $\text{cm}^2 \text{ molec.}^{-1}$ )				
	295 K	270 K	250 K	230 K	210 K
170	229	229	228	228	228
172	181	179	177	176	174
174	140	137	135	133	130
176	106	103	100	97.8	95.5
178	78.8	75.7	73.2	70.9	68.7
180	57.8	55.9	52.7	50.6	48.6
182	41.8	39.3	37.4	35.6	33.9
184	29.8	27.7	26.2	24.7	23.3
186	21.1	19.4	18.1	17.0	15.9
188	14.7	13.4	12.4	11.5	10.7
190	10.2	9.18	8.45	7.77	7.15
192	6.99	6.23	5.69	5.19	4.73
194	4.76	4.20	3.80	3.44	3.11
196	3.22	2.81	2.52	2.26	2.03
198	2.16	1.86	1.66	1.48	1.31
200	1.44	1.23	1.08	0.957	0.845
202	0.949	0.804	0.704	0.616	0.539
204	0.622	0.521	0.453	0.393	0.342
206	0.404	0.336	0.289	0.249	0.215
208	0.260	0.214	0.183	0.156	0.134
210	0.166	0.135	0.115	0.0972	0.0825
212	0.105	0.0844	0.0710	0.0598	0.0503
214	0.0652	0.0521	0.0435	0.0363	0.0303
216	0.0401	0.0317	0.0262	0.0217	0.0180
218	0.0243	0.0190	0.0156	0.0128	0.0105
220	0.0145	0.0112	0.00911	0.00741	0.00604
222	0.00845	0.00647	0.00522	0.00421	0.00340
224	0.00484	0.00366	0.00293	0.00234	0.00187
226	0.00271	0.00202	0.00160	0.00127	0.00100
228	0.00148	0.00109	0.000854	0.000670	0.000525
230	0.000783	0.000570	0.000442	0.000343	0.000226

### 3.1. Ambient Temperature (295 K)

At ambient temperature, the three compounds display continuous absorption with values ranging from  $1.8 \times 10^{-18}$  to  $10^{-24} \text{ cm}^2 \text{ molec}^{-1}$ , without any indications of structure in the spectrum. Results of other determinations (Hubrich and Stuhl, 1980; Molina and Molina, 1989; Orlando *et al.*, 1989; Allied-Signal Corporation, 1989) are presented in Figures 2–4 for comparison purposes.

For HCFC-123, the agreement between the four sets of data is relatively good in the 'atmospheric window' (near 200 nm), namely within  $\pm 10\%$ , but the differences increase for higher wavelengths (up to 50% at 230 nm).

For HCFC-141b, the agreement between all the measurements is good in the



Table IVb. Absorption cross-sections of HCFC-142b ( $\text{CH}_3\text{—CF}_2\text{Cl}$ ) averaged over the spectral intervals of  $500\text{ cm}^{-1}$  used in atmospheric modelling calculations for five selected temperatures (295, 270, 250, 230, 210 K)

No.	Wavelength (nm)	$\sigma(\lambda) \times 10^{21}$ ( $\text{cm}^2\text{ molec.}^{-1}$ )				
		295 K	270 K	250 K	230 K	210 K
43	169.5–172.4	205	204	203	202	201
44	172.4–173.9	156	154	152	150	148
45	173.9–175.4	128	125	123	120	118
46	175.4–177.0	103	99.6	97.2	94.8	92.4
47	177.0–178.6	81.2	78.1	75.6	73.3	71.0
48	178.6–180.2	63.5	60.5	58.3	56.1	54.0
49	180.2–181.8	49.2	46.5	44.5	42.5	40.6
50	181.8–183.5	37.5	35.1	33.3	31.7	30.1
51	183.5–185.2	28.1	26.1	24.6	23.2	21.8
52	185.2–186.9	20.9	19.2	18.0	16.8	15.7
53	186.9–188.7	15.3	13.9	12.9	12.0	11.1
54	188.7–190.5	11.2	10.1	9.31	8.58	7.92
55	190.5–192.3	7.83	7.01	6.41	5.86	5.36
56	192.3–194.2	5.50	4.88	4.42	4.02	3.64
57	194.2–196.1	3.80	3.34	3.00	2.70	2.44
58	196.1–198.0	2.61	2.27	2.03	1.81	1.62
59	198.0–200.0	1.76	1.51	1.34	1.19	1.05
60	200.0–202.0	1.17	0.995	0.874	0.769	0.676
61	202.0–204.1	0.761	0.641	0.559	0.487	0.425
62	204.1–206.2	0.486	0.405	0.350	0.303	0.262
63	206.2–208.3	0.307	0.254	0.217	0.186	0.160
64	208.3–210.5	0.190	0.155	0.132	0.112	0.0954
65	210.5–212.8	0.114	0.0917	0.0773	0.0651	0.0549
66	212.8–215.0	0.0668	0.0553	0.0445	0.0372	0.0311
67	215.0–217.4	0.0382	0.0301	0.0249	0.0206	0.0171
68	217.4–219.8	0.0208	0.0162	0.0133	0.0109	0.00892
69	219.8–222.2	0.0111	0.00853	0.00691	0.00560	0.00454
70	222.2–224.7	0.00565	0.00429	0.00344	0.00276	0.00221
71	224.7–227.3	0.00271	0.00202	0.00160	0.00127	0.00101

200 nm region (within the experimental accuracy), but for wavelengths greater than 210 nm, the values proposed by Orlando *et al.* and by the Allied-Signal Corporation became larger than those of the two other sets (up to a factor of 2 at 220 nm).

For HCFC-142b, the same good agreement is observed around 200 nm. In this case, the very first values proposed by Hubrich and Stuhl (1980) are much larger (up to a factor of 7 at 230 nm) for wavelengths greater than 210 nm.

The differences between these sets of measurements are difficult to explain in terms of their accuracy. The purity of the compounds used in this work has been checked very carefully, as explained in the experimental section. We do not have any indication of the level and the nature of the impurities in the products used in the other determinations.

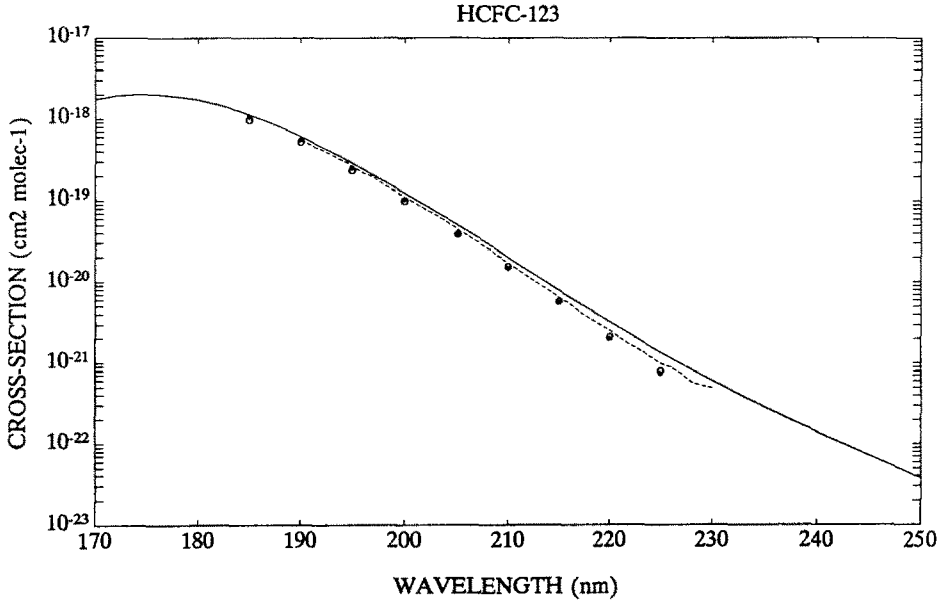


Fig. 2. Ultraviolet absorption cross-sections of  $\text{CF}_3\text{-CHCl}_2$  (HCFC-123) at 295 K, between 170 and 250 nm. — this work; ---- Orlando *et al.* (1989); • Molina and Molina (1989); ○ Allied-Signal Corporation (1989).

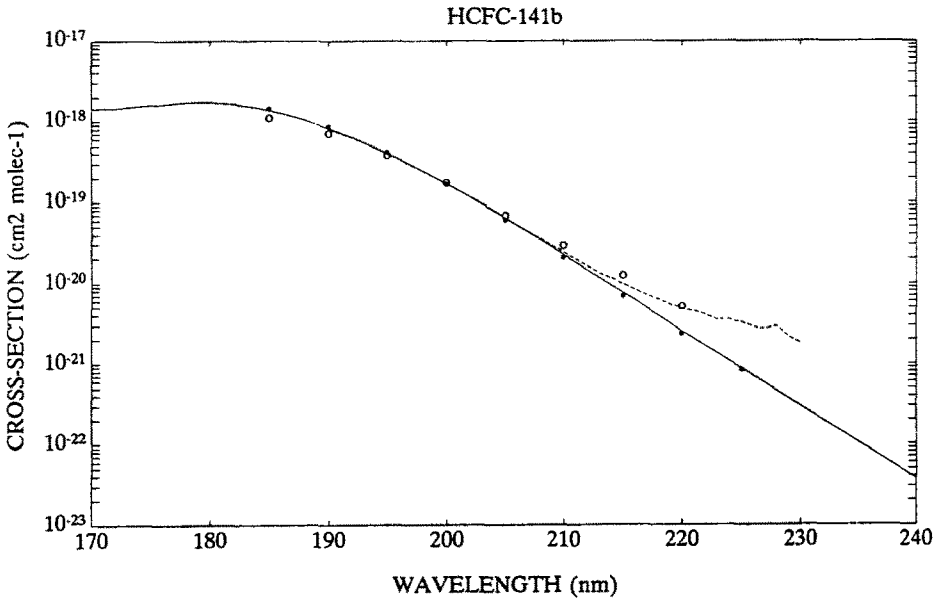


Fig. 3. Ultraviolet absorption cross-sections of  $\text{CH}_3\text{-CFCl}_2$  (HCFC-141b) at 295 K, between 170 and 240 nm. — this work; ---- Orlando *et al.* (1989); • Molina and Molina (1989); ○ Allied-Signal Corporation (1989).

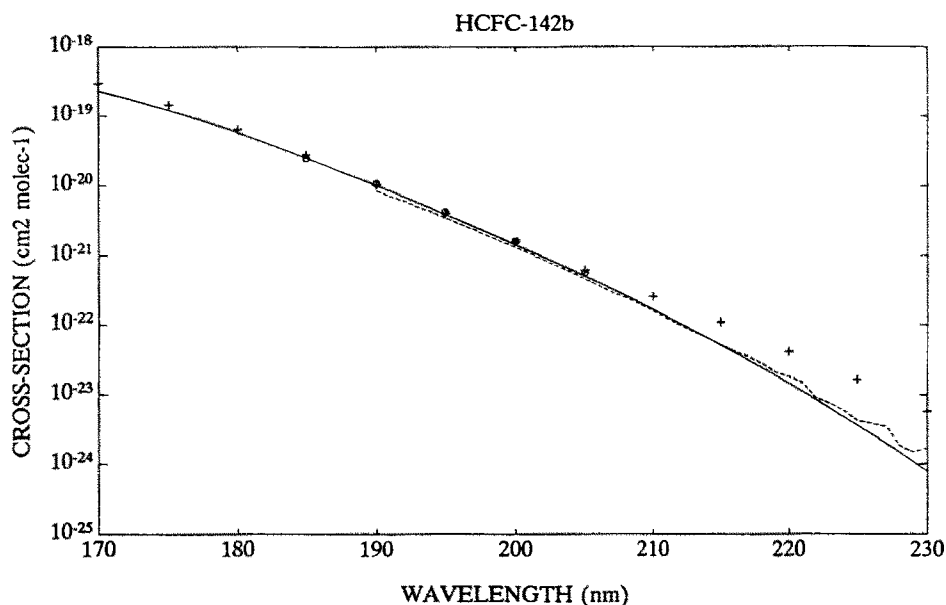


Fig. 4. Ultraviolet absorption cross-sections of  $\text{CH}_3\text{—CF}_2\text{Cl}$  (HCFC-142b) at 295 K, between 170 and 230 nm. — this work; --- Orlando *et al.* (1989); + Hubrich and Stuhl (1980); o Allied-Signal Corporation (1989).

### 3.2. Low Temperature (210–270 K)

Absorption cross-sections have been measured at three temperatures in the greatest range of pressure afforded by the vapour pressure conditions. The experimental conditions are presented in Table I. At low temperature, the absorption cross-sections show a temperature-dependence on both the wavelength and the chemical composition of the compound. The absorption cross-sections decrease with the temperature in the region of longer wavelengths and increase in the region of the maximum (around 170 nm for HCFC-123 and around 180 nm for HCFC-141b).

These effects are most significant at the lower temperature.

Figures 5–7 show the relative values of the absorption cross-section  $\sigma(T)/\sigma(295\text{ K})$  versus the wavelength relationships, for a given temperature and illustrate the effects mentioned above. Also in these figures are represented the relative absorption cross-section values calculated from the data proposed by Orlando *et al.* (1989) at ambient and low temperatures.

For HCFC-123, the temperature-dependences measured by Orlando *et al.* are smaller than those reported here in the region 190–205 nm. For wavelengths greater than 205–210 nm, it seems that their results became incoherent. In fact, the cross-section values at low temperatures are greater than those obtained at the ambient temperature (ratio greater than 1) which is not expected for similar measurements with other CFC (Simon *et al.*, 1988a, b; Hubrich and Stuhl, 1980; Chou *et al.*, 1977).

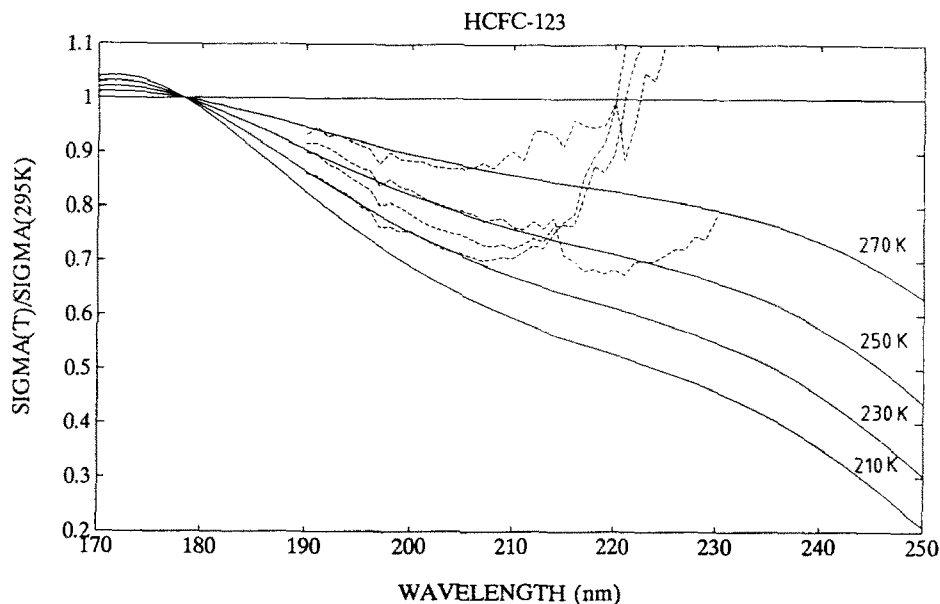


Fig. 5. Relative absorption cross-sections  $\sigma(T)/\sigma(295\text{ K})$  of  $\text{CF}_3\text{---CHCl}_2$  (HCFC-123) as a function of wavelength. — this work ( $T = 270, 250, 230, 210\text{ K}$ ); --- Orlando *et al.* (1989) ( $T = 263, 243, 223, 203\text{ K}$ ).

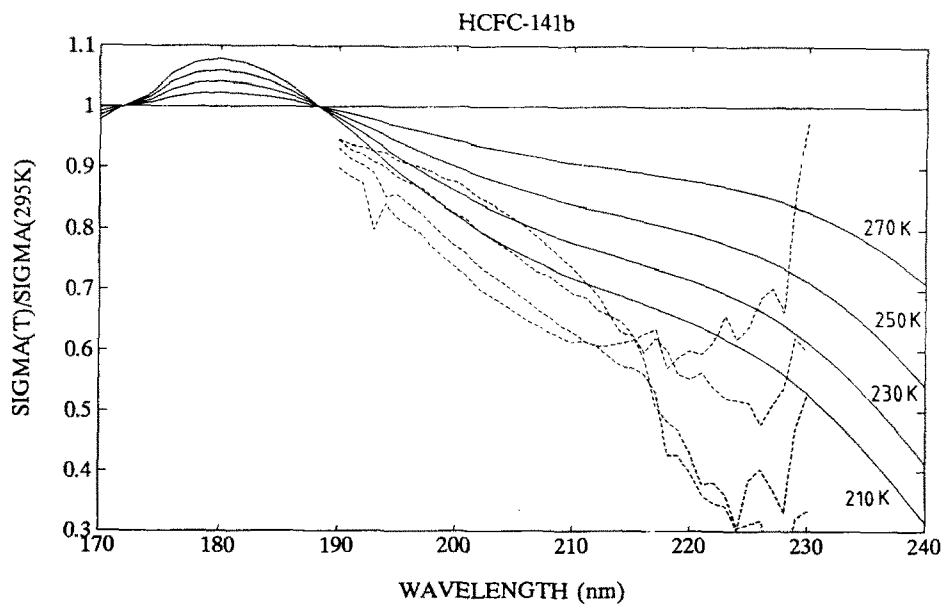


Fig. 6. Relative absorption cross-sections  $\sigma(T)/\sigma(295\text{ K})$  of  $\text{CH}_3\text{---CFCl}_2$  (HCFC-141b) as a function of wavelength. — this work ( $T = 270, 250, 230, 210\text{ K}$ ); --- Orlando *et al.* (1989) ( $T = 263, 243, 223, 203\text{ K}$ ).

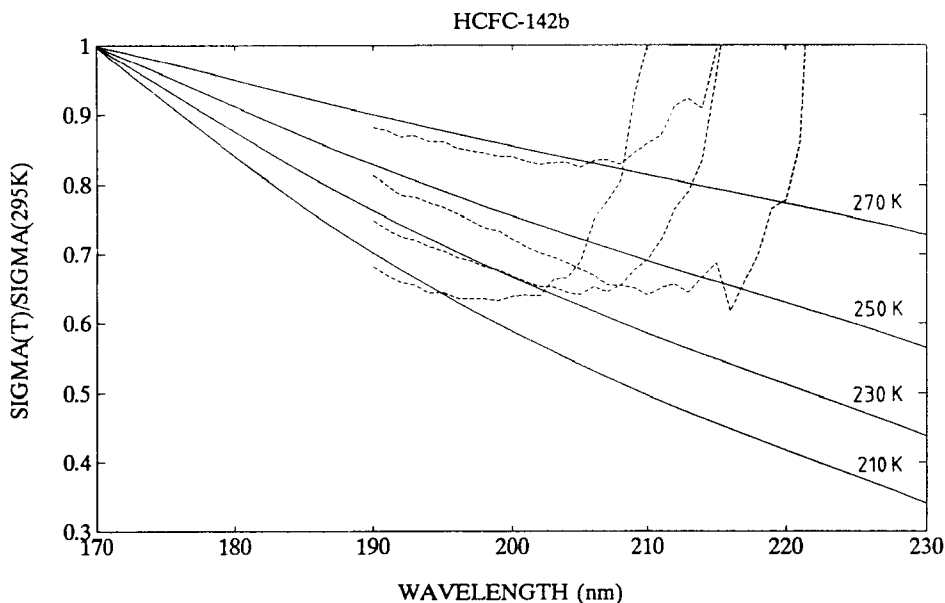


Fig. 7. Relative absorption cross-sections  $\sigma(T)/\sigma(295\text{ K})$  of  $\text{CH}_3\text{—CF}_2\text{Cl}$  (HCFC-142b) as a function of wavelength. — this work ( $T = 270, 250, 230, 210\text{ K}$ ); --- Orlando *et al.* (1989) ( $T = 263, 243, 223, 203\text{ K}$ ).

In the case of HCFC-141b, the temperature-dependences measured by Orlando *et al.* are greater than those reported in this work. The same inconsistencies in the observations can be seen in Figure 6 for wavelengths greater than 210 nm.

For HCFC-142b, the temperature-dependences are of the same order. Inconsistencies appear in the determination of Orlando *et al.* for wavelengths greater than 205 nm at 263 and 243 K, 200 nm at 223 K and 195 nm at 203 K.

Experimental conditions (transmissions lower than 10% or higher than 85%; incident and transmitted fluxes not measured in the same conditions of temperature) would explain these incoherences (see Section 2 and Figure 1).

For the three compounds, an exponential dependence of absorption cross-sections with respect to temperature at each wavelength is observed. This type of dependence has already been mentioned, and illustrated for similar compounds (e.g. Simon *et al.*, 1988a, b).

Numerical values interpolated through the absorption cross-section values obtained at three temperatures are presented in Tables II–IV for five selected temperatures (295, 270, 250, 230 and 210 K) which cover the usual atmospheric temperature conditions.

According to their exponential dependence versus temperature, the absorption cross-sections can be represented by an empirical function of temperature at each wavelength, thanks to the expression

$$\log_{10} \sigma(\lambda) = A(\lambda) + B(\lambda) \times T, \quad (1)$$

Table V. Parameters  $A_i$  and  $B_i$  for polynomial function (see formula (3) in the text)

$CF_3-CHCl_2$ (HCFC-123):	
$A_0 = -513.996354$	$B_0 = 1.757133$
$A_1 = 9.089141$	$B_1 = -3.499205 \times 10^{-2}$
$A_2 = -6.136794 \times 10^{-2}$	$B_2 = 2.593563 \times 10^{-4}$
$A_3 = 1.814826 \times 10^{-4}$	$B_3 = -8.489357 \times 10^{-7}$
$A_4 = -1.999514 \times 10^{-7}$	$B_4 = 1.037756 \times 10^{-9}$
$T$ range: 210–300 K	
$\lambda$ range: 182–250 nm	
$CH_3-CFCl_2$ (HCFC-141b):	
$A_0 = -682.913042$	$B_0 = 4.074747$
$A_1 = 12.122290$	$B_1 = -8.053899 \times 10^{-2}$
$A_2 = -8.187699 \times 10^{-2}$	$B_2 = 5.946552 \times 10^{-4}$
$A_3 = 2.437244 \times 10^{-4}$	$B_3 = -1.945048 \times 10^{-6}$
$A_4 = -2.719103 \times 10^{-7}$	$B_4 = 2.380143 \times 10^{-9}$
$T$ range: 210–300 K	
$\lambda$ range: 172–240 nm	
$CH_3-CF_2Cl$ (HCFC-142b):	
$A_0 = -328.092008$	$B_0 = 4.289533 \times 10^{-1}$
$A_1 = 6.342799$	$B_1 = -9.042817 \times 10^{-3}$
$A_2 = -4.810362 \times 10^{-2}$	$B_2 = 7.018009 \times 10^{-5}$
$A_3 = 1.611991 \times 10^{-4}$	$B_3 = -2.389065 \times 10^{-7}$
$A_4 = -2.042613 \times 10^{-7}$	$B_4 = 3.039799 \times 10^{-10}$
$T$ range: 210–300 K	
$\lambda$ range: 172–230 nm	

where the parameters  $A$  and  $B$  were determined by a polynomial least-square fit of the experimental data with respect to temperature and wavelength to obtain the following polynomial expressions

$$\log_{10} \sigma(\lambda, T) = A_0 + A_1 \lambda + \dots + A_n \lambda^n + (T - 273) \times (B_0 + B_1 \lambda + \dots + B_n \lambda^n). \quad (2)$$

The computed values of  $A$  and  $B$  are given in Table V. The values of absorption cross-sections calculated with expression (2) represent all the experimental results with differences smaller than 5%.

#### 4. Discussion

Photodissociation coefficients  $J$  for a given altitude  $z$ , zenith angle  $\chi$  and wavelength interval have been computed according to the relations:

$$\begin{aligned} J^z &= \sigma_\lambda q_\lambda(z), \\ q_\lambda(z) &= q_\lambda(\infty) e^{-\tau_\lambda(z)}, \\ \tau_\lambda(z) &= \int_z^\infty [n(O_2)\sigma(O_2) + n(O_3)\sigma(O_3) + n(\text{air})\sigma_{\text{scatt.}}] \sec \chi \, dz, \end{aligned} \quad (3)$$

Table VI. Photodissociation coefficients versus altitude

Z(km)	sec $\chi = 1$			sec $\chi = 2$		
	$J(\text{s}^{-1})$ $\sigma(295 \text{ K})^a$	$J(\text{s}^{-1})$ $\sigma = f(T)$	$J_{\text{rel}}$	$J(\text{s}^{-1})$ $\sigma(295 \text{ K})^a$	$J(\text{s}^{-1})$ $\sigma = f(T)$	$J_{\text{rel}}$
<i>HCFC-123 (CF<sub>3</sub>—CHCl<sub>2</sub>):</i>						
15	$9.236 \times 10^{-10}$	$5.973 \times 10^{-10}$	0.648	$2.300 \times 10^{-12}$	$1.495 \times 10^{-12}$	0.650
20	$1.169 \times 10^{-8}$	$7.724 \times 10^{-9}$	0.661	$2.149 \times 10^{-10}$	$1.407 \times 10^{-10}$	0.655
25	$7.380 \times 10^{-8}$	$5.133 \times 10^{-8}$	0.696	$5.273 \times 10^{-9}$	$3.612 \times 10^{-9}$	0.685
30	$2.887 \times 10^{-7}$	$2.098 \times 10^{-7}$	0.729	$5.549 \times 10^{-8}$	$3.974 \times 10^{-8}$	0.716
35	$7.649 \times 10^{-7}$	$5.941 \times 10^{-7}$	0.777	$2.912 \times 10^{-7}$	$2.223 \times 10^{-7}$	0.764
40	$1.475 \times 10^{-6}$	$1.229 \times 10^{-6}$	0.834	$8.655 \times 10^{-7}$	$7.118 \times 10^{-7}$	0.822
45	$2.149 \times 10^{-6}$	$1.909 \times 10^{-6}$	0.888	$1.562 \times 10^{-6}$	$1.375 \times 10^{-6}$	0.880
50	$2.689 \times 10^{-6}$	$2.461 \times 10^{-6}$	0.915	$2.158 \times 10^{-6}$	$1.960 \times 10^{-6}$	0.908
$\infty$	$6.195 \times 10^{-6}$					
<i>HCFC-141b (CH<sub>3</sub>—CFCl<sub>2</sub>):</i>						
15	$1.117 \times 10^{-9}$	$8.572 \times 10^{-10}$	0.767	$2.818 \times 10^{-12}$	$2.170 \times 10^{-12}$	0.770
20	$1.448 \times 10^{-8}$	$1.135 \times 10^{-8}$	0.784	$2.652 \times 10^{-10}$	$2.057 \times 10^{-10}$	0.776
25	$9.343 \times 10^{-8}$	$7.622 \times 10^{-8}$	0.816	$6.630 \times 10^{-9}$	$5.321 \times 10^{-9}$	0.803
30	$3.683 \times 10^{-7}$	$3.115 \times 10^{-7}$	0.846	$7.074 \times 10^{-8}$	$5.872 \times 10^{-8}$	0.830
35	$9.783 \times 10^{-7}$	$8.635 \times 10^{-7}$	0.882	$3.726 \times 10^{-7}$	$3.230 \times 10^{-7}$	0.867
40	$1.872 \times 10^{-6}$	$1.719 \times 10^{-6}$	0.918	$1.099 \times 10^{-6}$	$9.967 \times 10^{-7}$	0.907
45	$2.703 \times 10^{-6}$	$2.565 \times 10^{-6}$	0.949	$1.966 \times 10^{-6}$	$1.851 \times 10^{-6}$	0.941
50	$3.369 \times 10^{-6}$	$3.248 \times 10^{-6}$	0.964	$2.707 \times 10^{-6}$	$2.593 \times 10^{-6}$	0.958
$\infty$	$6.917 \times 10^{-6}$					
<i>HCFC-142b (CH<sub>3</sub>—CF<sub>2</sub>—Cl):</i>						
15	$8.687 \times 10^{-12}$	$4.828 \times 10^{-12}$	0.556	$2.202 \times 10^{-14}$	$1.227 \times 10^{-14}$	0.558
20	$1.154 \times 10^{-10}$	$6.585 \times 10^{-11}$	0.571	$2.089 \times 10^{-13}$	$1.177 \times 10^{-12}$	0.564
25	$7.710 \times 10^{-10}$	$4.707 \times 10^{-10}$	0.611	$5.339 \times 10^{-11}$	$3.192 \times 10^{-11}$	0.598
30	$3.176 \times 10^{-9}$	$2.064 \times 10^{-9}$	0.650	$5.864 \times 10^{-10}$	$3.718 \times 10^{-10}$	0.634
35	$8.884 \times 10^{-9}$	$6.291 \times 10^{-9}$	0.708	$3.214 \times 10^{-9}$	$2.224 \times 10^{-9}$	0.692
40	$1.790 \times 10^{-8}$	$1.398 \times 10^{-8}$	0.781	$9.915 \times 10^{-9}$	$7.610 \times 10^{-9}$	0.768
45	$2.738 \times 10^{-8}$	$2.336 \times 10^{-8}$	0.853	$1.861 \times 10^{-8}$	$1.569 \times 10^{-8}$	0.843
50	$3.848 \times 10^{-8}$	$3.397 \times 10^{-8}$	0.883	$2.714 \times 10^{-8}$	$2.387 \times 10^{-8}$	0.880
$\infty$	$1.827 \times 10^{-7}$					

<sup>a</sup> Temperature independent cross-section.

$J_{\text{rel}}$  = relative values  $J(T)/J(295 \text{ K})$

where  $\sigma$  are the absorption cross-sections,  $q_\lambda(z)$  and  $q_\lambda(\infty)$  are the solar irradiance at altitude  $z$  or extraterrestrial ( $z = \infty$ ),  $n$  are the number of particles per volume unit, for solar zenith angles of  $0^\circ$  and  $60^\circ$  (sec  $\chi = 1$  and 2), taking the values of  $\sigma(\text{O}_2)$ ,  $\sigma(\text{O}_3)$  from WMO (1986) and Kockarts (1976), of  $\sigma_{\text{scatt}}$  from Nicolet (1984), and the values of  $q_\lambda(\infty)$  from WMO (1986), and taking into account the actual values of cross-sections which correspond to the temperature conditions prevailing at a definite altitude.

A comparison of either temperature-dependent or independent photodissociation coefficients for different stratospheric altitudes (15 to 50 km) is presented in

Table VI where relative photodissociation coefficients  $J(T)/J(295)$  are given for the studied compounds.

Obviously, the effect is maximum in the low stratosphere and gradually decreases following the temperature profile in the stratosphere.

The value of the overall photodissociation coefficients between 15 and 35 km is mainly influenced by the 200–210 nm interval contribution due to the significant increase of the ozone optical depth in the stratosphere at wavelengths greater than 220 nm. In such conditions, a significant reduction of overall photodissociation coefficients is only to be expected in the case of compounds whose absorption cross-sections are strongly temperature-dependent in this wavelength interval.

Accordingly, important reduction factors are observed for HCFC-123 (up to 35%), for HCFC-142b (up to 45%), and, to a lesser extent, for HCFC-141b (up to 25%). The introduction of smaller photodissociation coefficients in atmospheric models theoretically increases the altitudes of photolysis and, therefore, changes the altitude profile of the considered halocarbons in the stratosphere. This effect could have minor atmospheric implications due to the fact that these compounds are relatively easily destroyed in the troposphere by reaction with OH radicals and, consequently, their lifetimes in the atmosphere are shorter than the fully halogenated halocarbons (global lifetime of 2 years for HCFC-123, 8.5 years for HCFC-141b, and 21 years for HCFC-142b) (Gillotay *et al.*, 1989a).

In conclusion, this work presents a complete and coherent set of experimental data showing a nonnegligible temperature-dependence of the absorption cross-sections and of the photodissociation coefficients of alternative chlorofluoroethanes. It gives fairly simple parametrical functions which can be used to approximate the absorption cross-section values with respect to temperature and wavelength within  $\pm 5\%$ .

Nevertheless, no major implication of the temperature-dependence of the absorption cross-sections of these compounds on the stratospheric photochemistry is expected because of the relatively short chemical lifetime of these species in the atmosphere.

### Acknowledgements

The authors wish to thank Drs G. Maertens and J. Franklin from Solvay S. A. for providing the studied compounds, Mr L. Dierickx who performed some of the measurements, and Mr E. Falise who performed the computer calculations of the photodissociation coefficients.

### References

- Allied-Signal Corporation, 1989, in WMO Report 20: Scientific Assessment of Stratospheric Ozone: 1989, Volume II, Appendix: AFEAS Report.  
Chou, C. C., Smith, W. S., Vera Ruiz, H., Moe, K., Crecentini, G., Molina, M. J., and Rowland, F. S.,



- 1977, The temperature dependences of the ultraviolet absorption cross-sections of  $\text{CCl}_2\text{F}_2$  and  $\text{CCl}_3\text{F}$ , and their stratospheric significance, *J. Phys. Chem.* **81**, 286–290.
- Gillotay, D., Simon, P. C., and Brasseur, G., 1989a, Absorption cross-section of alternative chlorofluoroethanes and potential effects on the ozone layer, *Planet. Space Sci.* **37**, 105–108. Corrigendum, *Planet. Space Sci.* **37**, 1025.
- Gillotay, D., Jenouvrier, A., Coquart, B., Merienne, M. F., and Simon, P. C., 1989b, Ultraviolet absorption cross-section of bromoform in the temperature range 295–240 K, *Planet. Space Sci.* **37**, 1127–1140.
- Hubrich, C. and Stuhl, F., 1980, The ultraviolet absorption of some halogenated methanes and ethanes of atmospheric interest, *J. Photochem.* **12**, 93–107.
- Kockarts, G., 1976, Absorption and photodissociation in the Schumann–Runge bands of molecular oxygen in the terrestrial atmosphere, *Planet. Space Sci.* **24**, 589–604.
- Molina, M. J. and Molina, L. T., 1989, in WMO Report 20: Scientific Assessment of Stratospheric Ozone: 1989, Volume II, Appendix: AFEAS Report.
- Montreal Protocol on Substances that Deplete the Ozone Layer, Final Act, 1987, United Nations Environment Programme.
- Nicolet, M., 1984, On the molecular scattering in the terrestrial atmosphere: an empirical formula for calculation in the homosphere, *Planet. Space Sci.* **32**, 1467–1468.
- Orlando, J. J., Burkholder, J. B., McKeen, S. A., and Ravishankara, A. R., 1989, The atmospheric fate of several hydrochloro-fluoroethanes 2. Temperature dependence of UV absorption cross sections, submitted for publication in *J. Geophys. Res.*
- Simon, P. C., Gillotay, D., Vanlaethem-Meuree, N., and Wisenberg, J., 1988a, Ultraviolet absorption cross-sections of chloro- and chlorofluoro-methanes at stratospheric temperatures, *J. Atmos. Chem.* **7**, 107–135.
- Simon, P. C., Gillotay, D., Vanlaethem-Meuree, N., and Wisenberg, J., 1988b, Temperature dependence of Ultraviolet absorption cross-sections of chlorofluoroethanes, *Ann. Geophysicae.* **6**, 239–248.
- WMO, 1986, Atmospheric ozone 1985, WMO Global Ozone Research and Monitoring Project, Report 16, Vol. I, pp. 355–367.